INTERNATIONAL JOURNAL OF MANAGEMENT SCIENCE AND ENGINEERING MANAGEMENT
https://doi.org/10.1080/17509653.2018.1500953

Evolutionary multi-objective optimization for bulldozer and its blade in soil cutting

Nada Barakat and Deepak Sharma

Mechanical Engineering, Indian Institute of Technology, Guwahati, India

ABSTRACT

The paper targets an optimal soil cutting operation by considering economic and productive aspects. Three realistic objectives and three problem-specific constraints are developed, and the optimization problem is solved using a hybrid evolutionary multi-objective optimization (EMO) technique. In this technique, a set of non-dominated solutions is generated by using an existing EMO technique, and then a few of them are selected for local search using the ε-constraint method. These selected solutions are used for starting independent local searches using *fmincon* solver of Matlab. Results demonstrate that the local searches have improved the non-dominated solutions a little, thereby suggesting a closeness of evolved solutions from EMO technique with true Pareto-optimal (PO) solutions. The PO solutions are further validated using experimental data from the literature. Overall, this study offers a platform to choose an appropriate solution from the set of PO solutions. Moreover, the post-optimal analysis demonstrates the commonality principle of few decision variables, which is followed by all PO solutions. The rest of the decision variables decipher important relationships that are responsible for trade-off among the PO solutions. The relationships are later used for preparing guidelines for a practitioner in selecting an appropriate solution for the optimal operation.

ARTICLE HISTORY
Received 26 February 2018
Accepted 12 July 2018

KEYWORDS
Engineering optimization; bulldozer; soil cutting; multi-objective; optimization; evolutionary algorithms; local search

1. Introduction

Real-world problems often consist of multiple objectives that are to be optimized simultaneously (Deb, 2001). When such problems are solved using any EMO technique, a set of PO solutions is generated that show trade-off among the objectives. These PO solutions provide multiple choices to a practitioner which otherwise is difficult to achieve when solving any single-objective optimization problem. Moreover, the multiple PO solutions offer a relative comparison among them so that an appropriate solution can be chosen. Furthermore, the post-optimal analysis (Deb & Srinivasan, 2006) can be performed to decipher important relationships among the objectives and decision variables. A commonality among the decision variables can be found that is followed by all PO solutions, which thus can be a design principle as demonstrated by (Baishya, Sharma, & Dixit, 2014; Barakat & Sharma, 2017b; Deb & Srinivasan, 2006; Sharma, 2010; Sharma & Barakat, 2018). Also, a set of decision variables can be found which are responsible for trade-off among the objectives. The important relationships among the objectives and decision variables can later be used for preparing guidelines for the practitioner. With those remarks, a real-world optimization problem is targeted in this paper from the domain of construction equipment in which the soil cutting operation is formulated for a bulldozer and its blade.

A bulldozer is construction equipment which has a tractor for supplying power and a metallic blade at its front for soil cutting. When the soil cutting operation is modeled for a bulldozer and its blade, an emphasis is given to make the operation economic and productive. The operation can be made economic when its variable cost can be reduced. The variable cost depends on the operating conditions which involve many parameters, such as power required from the bulldozer, the speed of the bulldozer, depth of a blade inserted in soil, dimensions of a blade, etc. The operation can be made productive when a bulldozer can finish the soil cutting operation as early as possible. However, any productive soil cutting operation with a large size blade operating at a larger speed and a higher cutting depth requires more power from the bulldozer.

In the literature, most of the earlier studies focused on determining the cutting force on a bulldozer blade at different cutting depths. For example, many analytical and numerical models have been developed that can determine the cutting force with the desired accuracy. The numerical models were developed using finite element methods (Abo-Elnor, Hamilton, & Boyle, 2004; Armin, Fotouhi, & Szyszkowski, 2014; Bentaher et al., 2013) and discrete element methods (Shmulevich, Asaf, & Rubinstein, 2007; Tsuji et al., 2012) which were found to be efficient by considering the effect of parameters, such as blade dimensions, cutting depth and cutting angle, etc. on the cutting force. However, the numerical models always demand higher computation time. On the other hand, the analytical models can determine the cutting force quickly on a blade with a reasonable accuracy. Under the umbrella of analytical models, two types have been developed which targeted either a two-dimensional or three-dimensional soil failure zone. The two-dimensional soil failure zone models have been used for wide blades. Reece (1964) proposed the two-dimensional model in which the fundamental equation of

CONTACT Deepak Sharma dsharma@iitg.ernet.in Mechanical Engineering, Indian Institute of Technology, Guwahati 781039, Assam, India

earthmoving mechanics was developed, which consists of resistance forces due to shear, cohesion, adhesion, and surcharge pressure between the blade and soil. Later, the weight of a soil wedge and inertia force were included into the fundamental equation of earthmoving mechanics by McKyes (1985). Qinsen and Shuren (1994) determined the cutting force on the wide blade by constructing a soil wedge. Various forces due to cohesion, adhesion and friction were considered between the blade and soil. Forces due to the soil pile accumulated in the front of the bulldozer blade were also taken into account. The three-dimensional soil failure zone models mainly targeted the narrow blades which are mainly used in tillage operations. Hettiaratchi and Reece (1967) developed the three-dimensional model for the fundamental equation of earthmoving mechanics, which was more accurate for the narrow blades.

Although earlier studies focused on determining the cutting force accurately, recent studies focused on making the soil cutting operation optimal. In (Barakat & Sharma, 2017a, 2017b, Sharma & Barakat, 2018), the operation is modeled using a bi-objective optimization formulation in which the cutting force was minimized, and the capacity of the bulldozer blade was maximized simultaneously. It was argued that minimizing the cutting force reduces overall resistance on the bulldozer that can reduce power requirement from the bulldozer. The reduction in power requirement can benefit in reducing the fuel consumption that can make the operation economic. The blade capacity objective was designed to make the operation productive so that a larger size blade can cut more soil in one pass. When the problem was solved using an EMO technique, it was found that a small size blade can optimize both the objectives. Although many interesting relationships among the objectives and decision variables were deciphered, variable blade dimensions were not among them. The present study develops more realistic objectives and problem-specific constraints so that dimensions of the blade and operating conditions can be taken as the decision variables for formulating the problem. The following are the contributions of this paper:

- Formulating a multi-objective optimization problem using three realistic objectives for a bulldozer and its blade in soil cutting operation.
- The Pareto-optimal solutions are generated using a hybrid evolutionary multi-objective algorithm in which the selected non-dominated solutions are used for starting the local searches.
- Deciphering relationships among the objectives and decision variables for a better understanding of the problem.
- Preparing guidelines for practitioner based on the obtained PO solutions and their post-optimal analysis.

The paper is organized into five sections. Section 2 presents the multi-objective optimization formulation in which the decision variables, objective functions, and constraints are developed for the soil cutting operation. Section 3 presents a hybrid EMO technique in which NSGA-II is coupled with the ε-constraint method. In Section 4, the PO solutions are presented, and various analyses is shown. The paper concluded in Section 5 with future work.

2. Proposed multi-objective optimization formulation

The soil cutting operation for bulldozer and its blade is formulated as a multi-objective optimization problem. The first objective is designed to minimize the power required from the bulldozer to overcome resistance and run it at the desired speed. The resistance in this operation is generated due to soil cutting and friction between the bulldozer and the ground. The only resistance that can be reduced is the resistance due to soil cutting in which enormous cutting force is generated between the blade and soil. As was argued in (Barakat & Sharma, 2017a), any reduction in power requirement signifies less fuel consumption that can make this operation economic. The second objective is designed to minimize the number of passes to cut a fixed volume of soil. The third objective is developed to minimize the time required to cut soil in one pass such that the blade of the bulldozer becomes filled with soil (Barakat & Sharma, 2017c). The second and third objectives are designed to make the operation productive. The second objective signifies overall productivity by finishing the operation in fewer passes, that requires large power requirement. The third objective signifies local perspective of productivity of the operation by filling the blade in less time. It conflicts with the overall productivity of the operation when a small size blade is used that can result in a greater number of passes. Also, it conflicts with larger power requirement objective when a small size blade is used at a higher depth of cut.

Seven decision variables are used to develop the objective functions. The decision variables are the cutting depth (D), the cutting angle (α), the velocity (v), the blade width (B), the blade height (H), the blade curvature radius (R), and the blade curvature angle (θ). Three problem-specific constraints are also developed that limit the required power to overcome ()the cutting force, limiting force generated on the blade in order to avoid its failure, and achieving the desired production rate. The proposed formulation is given in (1).

$$\begin{array}{lcl}
\text{Minimize} & P, & (\textit{Power}),\\
\text{Minimize} & N, & (\textit{Number of passes})\\
\text{Minimize} & T, & (\textit{Time}),\\
\text{subjectto} & P_R \geq 0, & (\textit{Remaining power}),\\
 & F \leq F_{max}, & (\textit{Blade failure}),\\
 & P_d \geq P_{d_{min}}, & (\textit{Production rate}),\\
 & 0.01 \leq D \leq 0.5, & (\textit{Decision variables}),\\
 & 0.785 \leq \alpha \leq 1.309,\\
 & 0.278 \leq v \leq 1.389,\\
 & 3 \leq B \leq 5,\\
 & 1 \leq H \leq 2.5,\\
 & 0.9 \leq R \leq 1.5,\\
 & 1.047 \leq \theta \leq 1.309.
\end{array} \tag{1}$$

2.1. *Objective function-1: power requirement (P)*

The first objective function is minimizing the power required to overcome resistance due to the cutting force (F) (Sharma & Barakat, 2018), which is given as

$$P = Fv \tag{2}$$

The cutting force model developed by Qinsen and Shuren (1994) is adopted in this paper for determining F. The details of this model is given in the Appendix.

2.2. *Objective function-2: number of passes (N)*

The second objective function is designed to minimize the number of passes that are required to cut a fixed volume of soil. It can only happen when the larger size blades are used at higher cutting depth. However, it can increase the power requirement from the bulldozer. The number of passes (N) is determined as

$$N = \frac{V_{max}}{V}, \tag{3}$$

where V_{max} is the fixed volume of soil to be cut, and V is the blade capacity that is calculated from the geometry of the blade as shown in Figure 1. The blade capacity (Sharma & Barakat, 2018) is determined as

$$V = V_1 + V_2 + V_3 + V_4, \tag{4}$$

where V_1 is the volume of (fde), V_2 is the volume of (afg), V_3 is the volume of (abdg), and V_4 is the volume of soil inside the arc (ab). These soil pile volumes are determined as

$$\begin{aligned} V_1 &= 0.5B\left(H + 2Dtan\varphi_o\right)^2 \cot\varphi_o, \\ V_2 &= 2BD^2 \tan\varphi_o, \\ V_3 &= DBH(\cot\alpha + \cot\beta), \\ V_4 &= 0.5B\theta R^2 - \left(0.5R^2 \sin\theta\right) \end{aligned} \tag{5}$$

2.3. *Objective function-3: time required to fill the blade (T)*

The third objective is to minimize the time that is required to fill the blade in one pass (Sharma & Barakat, 2018). It can only be done when a small-sized blade is used at higher cutting depth. However, a smaller size blade needs many passes to cut a fixed volume of soil. Moreover, the blade will experience a large cutting force at higher values of (D) which thus require more power from the bulldozer. It is calculated as

$$T = \frac{L}{v} \tag{6}$$

where L is the distance traveled by the bulldozer to fill the blade with soil in one pass. Here, the volume cut by the blade is equal to BDL that should be equivalent to the blade capacity. Therefore, $L$is calculated as

$$L = \frac{V}{BD} \tag{7}$$

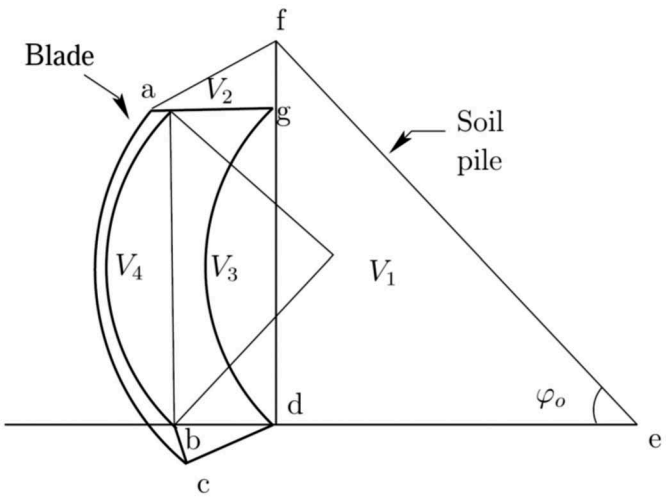

Figure 1. Blade capacity is determined from the geometry of the blade (Sharma & Barakat, 2018).

2.4. *Constraints*

Three problem-specific constraints are developed for the soil cutting operation. The first constraint is designed for the remaining power of the bulldozer (Sharma & Barakat, 2018). Since $P_R \geq 0$, it signifies that the bulldozer is able to overcome resistance due to the cutting force. The first constraint is given as

$$P_R = 0.85\ P_{bull} - P \geq 0 \tag{8}$$

Here, $P_{bull}$is the rated power of the bulldozer which is assumed to be operated at an efficiency of 85%.

The second constraint is developed for limiting the cutting force in order to avoid the blade failure. It is given as

$$F \leq F_{max} \tag{9}$$

Here, F_{max} is the force a blade can withstand. It is set to 700kN.

The third constraint is developed to achieve a desired rate of production. The production rate is defined as the rate of soil cut by a blade in one pass. The production rate is given as

$$P_d = \frac{V}{T} \geq P_{d_{min}} \tag{10}$$

where $P_{d_{min}}$ is the minimum limit on the production rate that is assumed to be $P_{d_{min}} = 0.01\ \text{m}^3$.

3. Hybrid EMO procedure

A hybrid EMO procedure is adopted in this paper to solve the three-objective optimization problem given in (1). In the literature, many hybrid EMO procedures exist that target to improve convergence of optimization algorithms (Coello Coello, Lamont, & Veldhuizen, 2007). In general, the local searches are coupled with the existing EMO techniques. Since there are various ways these local searches can be executed, the performance of the existing hybrid EMO techniques is found to be different. For example, the local search can be executed in every iteration on every solution of EMO technique (Kumar, Sharma, & Deb, 2007; Sharma, Kumar, Deb, & Sindhya, 2007), but it will be computationally expensive. Also, the local search can be executed on selected solutions of EMO techniques in every or after few generations (Deb, Miettinen, & Sharma, 2009; Sindhya, Miettinen, & Deb, 2013), but the effective guiding rules for variety of multi-objective optimization problems need to be devised. In this procedure, one of the benchmark

EMO techniques, which is as known as elitist non-dominated sorting genetic algorithm (NSGA-II) (Deb, Pratap, Agarwal, & Meyarivan, 2002), is chosen to run for a fixed size of population and generations. Thereafter, few solutions are chosen from the non-dominated front evolved by NSGA-II, and the local search is applied on them. The $\varepsilon-$ constraint method is chosen for local search because it is reported by Miettinen (1998) that if the primary objective is minimization, the $\varepsilon-$ constraint method can generate the PO solution by altering the upper bounds of constraints formed from other objectives.

The following definitions are used for the concept of dominance and the Pareto-optimality.

Definition 3.1: Given two solutions $x(1),\ x(2) \in \Omega$ (feasible search space), $x(1)$ is said to dominate $x(2)$, denoted by $x(1) \prec x(2)$, if $f_i(x(1)) \leq f_i(x(2))$, for every $i \in \{1,\ 2, \ldots, m\}$, and $f_j(x(1)) < f_j(x(2))$, for at least one objective $j \in \{1,\ 2, \ldots, m\}$ for minimization of all objective functions.

Definition 3.2: A solution x^* is said to be a non-dominated solution, iff there is no x in the given population such that$x \prec x^*$.

Definition 3.3: A solution x^{**} is said to be the PO solution, iff there is no $x \in \Omega$ such that $x \prec x^{**}$.

NSGA-II (Deb et al., 2002) is presented in Alg. 1. NSGA-II starts with initializing the population randomly. The solutions are then evaluated by determining the objective functions and constraints values. The non-dominated sorting and crowding distance operators are then used to assign fitness/rank to each solution of the initial population. The constraint-dominance definition is used for determining the rank of a solution. In this definition, a solution i is said to constrained-dominate a solution j, if any of the following conditions is true. (1) Solution i is feasible and solution j is not. (2) Solutions i and j are both infeasible, but solution i has a smaller overall constraint violation. (3) Solutions i and j are feasible and solution i dominates solution j. In non-dominated sorting, the solutions are sorted in different fronts that represent the rank of the solution. Any two solutions lying in the same front signifies the same rank. In order to differentiate same ranked solutions, the crowding distance is applied in which the crowding of a solution is determined with respect to its neighbors in the same front. The corner solutions of every front are assigned with a higher crowding distance value. NSGA-II then enters into the standard loop of generation by checking the condition on maximum allowed generation (T). Inside the loop, the constraint binary tournament selection is applied in which two randomly selected solutions from the population, now referred to as parent population P_t in t-th generation, are selected and their ranks are compared. The solution with a better rank gets selected in the mating pool. If both solutions have the same rank, then the solution with a higher crowding distance value is selected for the mating pool. The tie is broken arbitrarily. The binary tournament selection operator is applied twice on the population to make the mating pool of size$N$. The simulated binary crossover operator is then applied to randomly selected two solutions to create two offspring. The polynomial mutation is then applied to both offspring. The new population created after crossover and mutation is referred as offspring population Q_t. The non-dominated sorting operator is then applied to the combined population $(P_t \cup Q_t)$ to sort these solutions in different fronts. In the environment selection, one by one these fronts are copied to the next generation population P_{t+1} until its size is equal to N. If the last front that will be included has more solutions than the remaining size of P_{t+1}, the solutions are selected based on crowding distance in descending order of its value. This completes one generation of NSGA-II. After termination, NSGA-II evolves a set of non-dominated solutions.

Algorithm 1: NSGA-II algorithm

Input: Population size (N), maximum generations (T), crossover probability, mutation probability, generation counter (t = 0)

Output: Pareto-optimal solutions (P_{t+1})

Initialize random population P_t;

Evaluate P_t;

Assign rank using non-dominated sorting operator and diversity using crowding distance operator to P_t

while Generation counter $t < T$ do

$P_t^{'}$: = Selection (P_t) using crowded tournament selection operator;

Q_t: = Variation ($P_t^{'}$) using simulated binary crossover operator and polynomial mutation operator;

Evaluate Q_t;

Merge population $R_t = (P_t \cup Q_t)$;

Assign rank using non-dominated sorting operator and diversity using crowding distance operator to R_t;

P_{t+1}: Choose best N solutions from R_t based on rank and crowding distance;

$t = t + 1$;

end while

In the hybrid procedure, a few solutions from the set of non-dominated solutions are selected, and then the local search is applied on them using the $\varepsilon-$ constraint method. In this method, one objective among the three objectives given in (1) is considered as primary objective and other objectives are made constraints. For example, if an objective on power (P) is kept as a primary objective, then the constraint on the number of passes is made as $N \leq \epsilon_N$, and the constraint on the time is made as $T \leq \epsilon_T$. The objective on power and two constraints on N and T are then added with the constraints and decision variables of (1). The resulting single objective problem is solved using *fmincon* solver of Matlab 2016b® wherein the sequential quadratic programming (SQP) technique is chosen.

For executing the local search, values of ϵ_N and ϵ_T have to be assigned. Since few non-dominated solutions are chosen for the local search, their N and T values are assigned accordingly. For example, a non-dominated solution is evolved with values of objective as $(P_o,\ N_o, T_o)$ and decision variables as $(D_o, \alpha_o,\ \nu_o,\ B_o,\ H_o,\ R_o,\ \theta_o)$. In this case, values are assigned as $\epsilon_N = N_o$ and $\epsilon_T = T_o$. Moreover, SQP technique starts from $(D_o, \alpha_o,\ \nu_o,\ B_o,\ H_o,\ R_o,\ \theta_o)$, instead of some random values of decision variable. This can help SQP method to converge quickly to the true PO solution.

4. Results and discussion

For solving the multi-objective optimization problem, few of the parameters of NSGA-II are kept constant, e.g. population size is kept at 500, maximum generations are 500, the

Table 1. The mid-stiffness clay soil parameters in SI units. Units of C_o, Cand $A_d$are in (N/m^2).

γ_o	γ	C_O	C	δ	A_d	β	φ_o	φ
640.74	1601.85	1019.715	2039.43	21.6	0	23	30	27

probability of crossover is 0.9, crossover operator index is 20, the probability of mutation is 0.14286 (1/no. of variables), and mutation operator index is 20. The results are obtained for mid-stiffness clay soil, and its physical parameters are presented in Table 1. The bulldozer flywheel power is taken as P_{bull} = 227.438 kNm/s. The fixed volume of soil to be cut is set as V_{max} = 200 m^3.

4.1. *Pareto-optimal solutions*

Figure 2 shows the obtained PO solutions. For discussion, these solutions are categorized into three groups. The first group of obtained PO is referred as the surface solutions (blue color symbols) in which most of the solutions are generated at lower P values. The second group of solutions (black color filled symbols) is referred as the knee-solutions that show a decent trade-off among the objectives. The third region is referred as the extension solutions (green color symbols) in which the solutions do not show much trade-off between T and N, but objective P increases to its higher value. Three extreme solutions are also shown in the same figure wherein minimum P is represented by solution $a1$, minimum T is represented by solution $z1$, and minimum N is represented by solution $e1$.

The scatter plots for three objectives are shown in Figure 3. Since different colors for the symbols are used, three groups of the obtained PO solutions can be distinguished. The surface solutions are generated with lower P values. The same solutions show trade-off between N and T (refer Figure 3(c)) in which these solutions are generated over a wide range of N and T objectives. The second group is made of the knee-solutions, which is always important for a practitioner or decision maker. It is because the solutions show a decent trade-off among the posed objectives in this region. The solutions that are lying away from this region show any gain in one objective with a higher loss in another objective. The extension solutions are generated with lower N and T values (refer Figure 3(a,b)). However, higher P values can be observed.

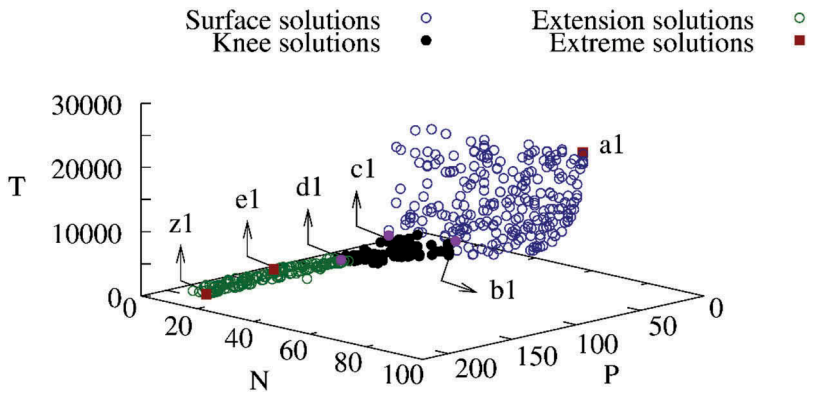

Figure 2. The obtained PO solutions from NSGA-II are presented. The solutions are categorized into three groups. Different colors are used for distinguishing the solutions lying in three groups. The unit of P and T are kN.m/s and s, respectively.

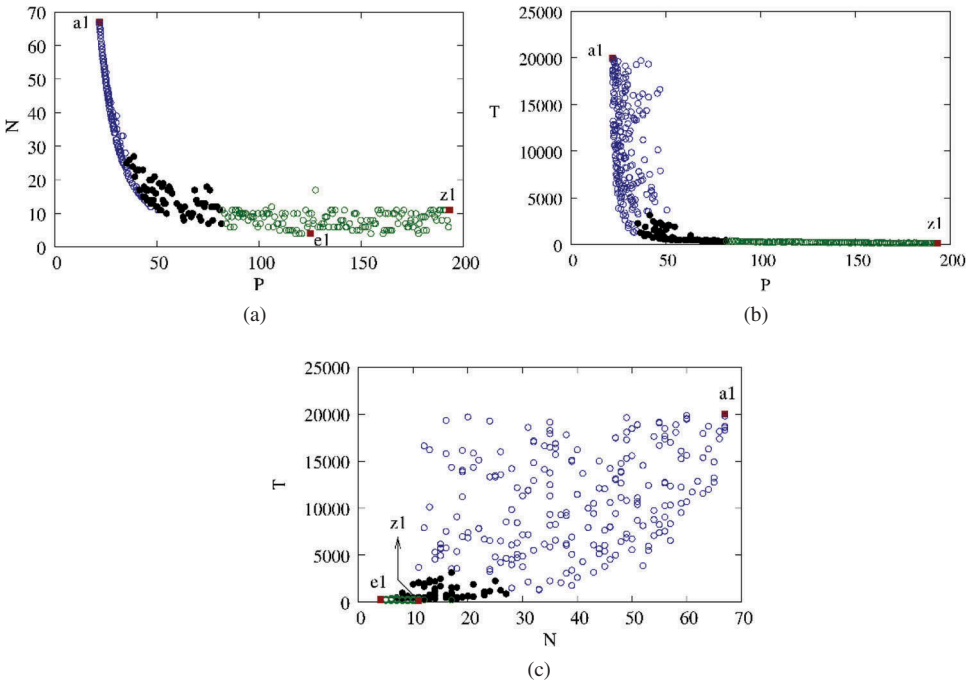

Figure 3. The scatter plots for three objectives are presented in which the relationships among the objectives are shown for three groups of the obtained PO solutions.

Few non-dominated solutions are then selected that are shown in Figure 2 for executing the local search using the $\varepsilon-$ constraint method. Solution '$a1$' representing minimum P, solution '$z1$' representing minimum T, and solution '$e1$' representing minimum N are selected for the local search. Other three solutions ($b1$, $c1$, $d1$) are selected to get one representation from each of the three groups of solutions, that are surface solutions, knee-solutions, and extension solutions. These solutions are selected at random from their respective group. The *fmincon* solver using the sequential quadratic programming technique starts from the selected non-dominated solutions as discussed in section 3. Table 2 presents NSGA-II solutions and the improved solutions using the $\varepsilon-$ constraint method. It can be seen that one objective among the three objectives in (1) is chosen as a primary objective one by one and rest of the objectives are made constraint. A marginal difference in the values of P and T objectives can be seen among the solutions. The $\varepsilon-$ constraint method was able to improve NSGA-II solutions by showing a smaller difference in the values of the decision variables from their original values obtained from NSGA-II. Since in (3), a nearest integer value of ratio is considered for determining$N$, the smaller changes in the decision variables values did not change the integer value of N. Therefore, N remains same for the solutions obtained using the $\varepsilon-$ constraint method.

It is known that NSGA-II and $\varepsilon-$ constraint method generated the PO solutions in different ways. EMO techniques simultaneously optimize the objectives and generated the PO solutions in one run. On the other hand, the $\varepsilon-$ constraint method converted the multi-objective optimization problem into the single-objective optimization problem by considering other objectives as constraints. The challenge is setting different values of ε_N and ε_T. This issue has been handled by considering the solutions from NSGA-II in this paper. Otherwise, it is difficult to set appropriate values of ε_N and ε_T which can generate well-distributed PO solutions. The task is even more difficult for the given problem due to the nature of the PO front showed in Figure 2. Moreover, *fmincon* solver has to run from different starting points to generate enough solutions to represent the PO front of the given problem. Nevertheless, the local search using the $\varepsilon-$ constraint method was able to generate marginally better solutions than NSGA-II.

The statistical performance analysis is performed for NSGA-II for which the NSGA-II is run for 30 times from different initial populations. The performance is observed by using the hypervolume (HV) indicator. It measures the hypervolume of that portion of the objective space that is weakly dominated by an approximate set A. This indicator gives the idea of spread quality and has to be maximized. Table 3 presents statistical HV indicator values for different crossover probability. It can be seen that the performance of NSGA-II remains similar.

4.2. *Post-optimal analysis*

The post-optimal analysis of the obtained PO solutions is now performed. The analysis is presented to find new and innovative design principles or relationships that can be used for deeper understanding of the problem as demonstrated for many engineering optimization problems in (Baishya et al., 2014; Barakat & Sharma, 2017b; Deb & Srinivasan, 2006; Sharma, 2010; Sharma & Barakat, 2018). Moreover, some guidelines can also be made for the practitioners involved in decision-making for the bulldozer and its blade. It is always interesting to reveal the common design principles that are responsible for generating the PO solutions. Also, some dissimilar relationships can be extracted that are responsible for trade-off among PO solutions.

The obtained PO solutions are shown in Figure 4 in which some decision variables are responsible for trade-off among the solutions, and others decipher the commonality principle for generating the PO solutions. It can be seen from D-R and D-θ plots that for all obtained solutions θ and R decision variables are evolved at their lowest bounds. This suggests a commonality principle that a solution can be the PO solution when θ and R are fixed at their lowest values.

Other decision variables are responsible for trade-off among the solutions. The surface solutions are evolved with lowest B and v. The range of D for these solutions is small, lying between (0.01, 0.183) m. Similarly, the range α of lies in between (0.78, 0.95). A wide range of H can be seen for the surface solutions which vary from 1 to 2.48 m.

Table 2. The solutions obtained from NSGA-II and $\varepsilon-$ constraint method are presented.

Solutions	NSGA-II solutions (P, N,T)	$\varepsilon-$ constraint solutions (P, ε_N, ε_T)
a1	(21.936, 67, 19999.92)	(21.935, 67, 19984.01)
b1	(33.623, 27, 2849.314)	(33.349, 27, 2854.859)
c1	(50.859, 11, 2907.186)	(50.859, 11, 2907.186)
d1	(83.584, 9, 362.356)	(83.584, 9, 362.356)
e1	(125.068, 4, 286.786)	(125.068, 4, 286.786)
z1	(193.231, 11, 134.563)	(193.068, 11, 134.353)
Solutions	$\varepsilon-$ constraint solutions (ε_P, N, ε_T)	$\varepsilon-$ constraint solutions (ε_P, ε_N, T)
a1	(21.935, 67, 19984.01)	(21.935, 67, 19971.36)
b1	(33.605, 27, 2854.859)	(33.623, 27, 2849.314)
c1	(50.822, 11, 2924.49)	(50.859, 11, 2907.186)
d1	(83.585, 9, 362.414)	(83.584, 9, 362.356)
e1	(125.198, 4, 286.611)	(125.068, 4, 286.786)
z1	(193.322, 11, 134.2105)	(193.322, 11, 134.176)

Table 3. Statistical HV indicator values for different crossover probabilities.

	1		0.9		0.8		0.7	
p_c	Mean	Std. Dev.	Mean	Std. Dev.	Mean	Std. Dev.	Mean	Std. Dev.
	9.67e-01	2.3e-04	9.67e-01	1.8e-04	9.67e-01	2.6e-04	9.67e-01	2.3e-04
p_c	0.6		0.5		0.4		0.3	
	9.67e-01	2.4e-04	9.67e-01	1.3e-04	9.67e-01	1.1e-04	9.67e-01	2.1e-04

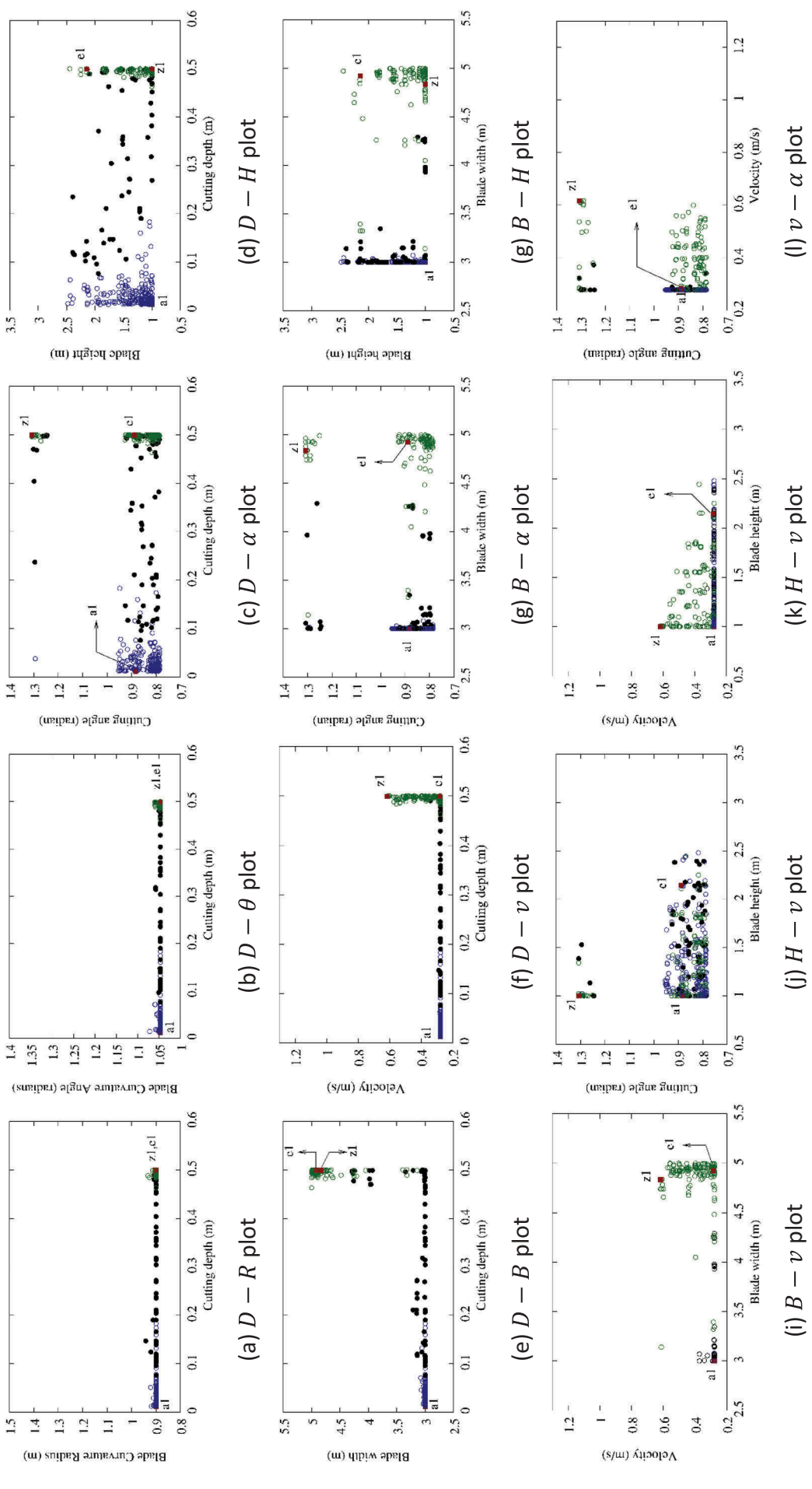

Figure 4. The scatter plots of the obtained PO solutions for all decision variables are presented. Two decision variables show commonality principle for generating the PO solutions. The rest of five decision variables are responsible for trade-off among the objectives.

It can be observed that the dimension of the blade changes only for different H values and other decision variables for blade dimension are evolved at their lower bounds. Since these solutions are evolved with lower values of D, it can be justified that these solutions are corresponding to lower P values as observed in Figure 2. For the same set of solutions, a wide range of T and N is also observed. It is because when a small size blade, meaning H is small, is used with lower D, it can become filled with soil quickly. However, this blade can take many passes to cut the fixed volume of soil. In contrast to this, a larger size blade with higher H is used; it can take more time to become filled with soil. However, the operation can be completed in fewer passes.

For the knee-solutions, a wide range of D from 0.07 to 0.5 m can be seen. The range of α is also widened from 0.78 to 1.3. The dimensions of the blade are also varied which can be observed from the ranges of H and B. It means that different blade dimensions are evolved which are operated at different D and α values. Since D is varying from its lower limit to upper limit, different sized blades show trade-off among all objectives. For example, a smaller blade at lower D takes more time to become filled compared to larger D. In this case, N remains the same but with larger D, the soil cutting operation can be finished early but requires more power from the bulldozer. Any larger blade with larger D can finish the operation relatively early against the lower D. However, the larger blade takes less N but higher P values to finish the soil cutting operation. All observations are in line with the knee-solutions of Figure 2, which showed a decent trade-off among the objectives.

For extension solutions, the decision variables B, H, v, and α vary from their lower to upper limits. Moreover, D remains at its upper bound of 0.5 m. This observation suggests that a wide range of blades is evolved for these solutions that have been used at higher D and all ranges of v and α. This is the reason that higher P values are observed in Figure 2 with less T and N.

4.3. *Guideline for practitioner*

The obtained PO solutions and their post-optimal analysis offer a platform to make guidelines for the practitioner. From Figure 2, it clear that the practitioner has three wide choices for selecting an optimal solution in practice. For example, lower P-value solution can be chosen from the surface solutions. On the other hand, the extension solutions offer lower N and T values. The knee-solutions offer a decent trade-off among the objectives for selection.

In case the group of the surface solutions is chosen by the practitioner, one PO solution has to be chosen from many solutions having trade-off between N and T. As can be seen from Figure 3(c), solution $a1$ corresponds to minimum P but with very large N and T. If any solution with lower T value is chosen, then approximately $N = 30$ passes are required to finish the soil cutting operation. It is because this solution is evolved with a lower value of H and D (refer Figure 4(d)). Thus, a small size blade is used for soil cutting at lower D. If a solution with lower N is chosen, then approximately 3700 s are required to fill the blade with soil. It means that a larger sized blade is used at lower D to finish the soil cutting task.

The next group, which can be chosen by the practitioner, is the extension solutions. These solutions correspond to lower N and T objective values but with higher P values. This is because medium to larger size blades are used at higher D and v for soil cutting, which can be seen from Figure 4(f). The solutions $e1$ and $z1$ belong to this group. The range of T is from 146 to 250 s, and the range of N is 6 to 13 for both solutions. Solution $z1$ corresponds to minimum T, but P is relatively high compared to solution $e1$. This is due to the larger-sized blade with larger D and v having evolved for solution $z1$ against medium-sized blade at the same operating condition for solution $e1$. Thus, the practitioner can choose $e1$ over $z1$. However, a solution with lowest P from the group of extension solutions can be chosen since the ranges of T and N are small.

The group of the knee-solutions is always preferable to the practitioner. This is because all solutions under this group show a decent trade-off among all objectives. The solutions are evolved with the smaller to larger size blades that are operated from lower to higher D values and moderate v range. The P values are not high, and the operation can finish in a reasonable range of N and T. In this group, the soil cutting operation can be finished early if the larger-sized blade is used at higher D but at the expense of higher P values. Otherwise, a smaller blade with lower D and moderate v can be used.

From the above discussion, it is clear that once a practitioner chooses the appropriate group of solutions, then one PO solution can be chosen. This study offers many choices to the practitioner for relative comparison and final selection of an appropriate solution. In practice, a set of bulldozer blades is available for performing the soil cutting. An appropriate blade and the operating condition can be found using the plots shown in Sections 4.1 and 4.2. For example, a suitable blade can be chosen from the evolved dimensions of the blade of the PO solution. The blade is then used with the evolved optimal operating conditions so that the desired objective function values can be achieved.

4.4. *Parametric analysis on constraints limits*

In this section, parametric analysis of constraints limits is performed to observe any change in the obtained PO solutions. It can be observed that the values of F_{max} and P_{dmin} in (1) are set, and the PO solutions are generated. However, these values can be altered by the practitioner for which another set of the PO solutions can be evolved. First, the current limit on the production rate is changed to $P_{dmin} = 0.2$ m^3/s. It can be seen in Figure 5 that one set of PO solutions is now feasible. For these solutions, the post-optimal analysis remains the same as presented in Section 4.2. An interesting observation is that any new run of NSGA-II for the modified multi-objective optimization problem with $P_{dmin} = 0.2$ is not required because the PO solutions can directly be identified. A similar observation can be seen in Figure 6 in which F_{max} is set as 120 kN. In this case also, one set of solutions becomes the PO solutions for which NSGA-II has not been run, and the PO solutions are identified.

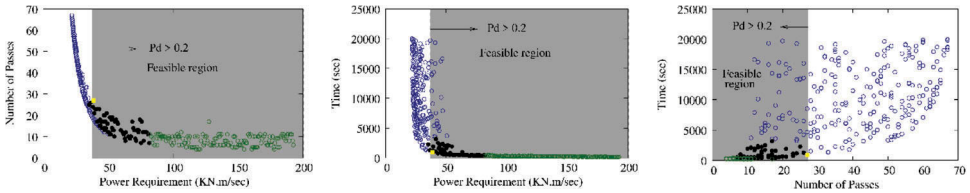

Figure 5. The obtained PO solutions when $P_d \geq 0.2$ m^3/s is set.

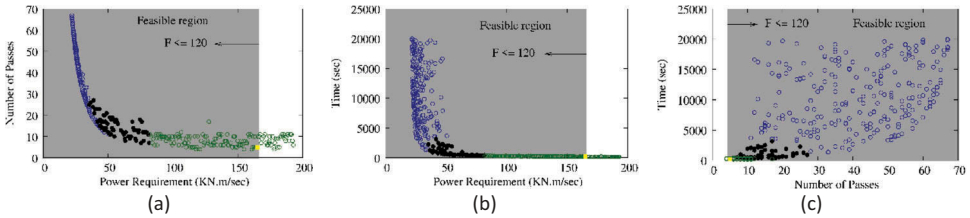

Figure 6. The obtained PO solutions when F ≤ 120 kN is set.

Table 4. The parameters of King et al. (2011) for experimental validation of solutions are presented.

γ_o (kg/m^3)	γ (kg/m^3)	C_o (N/m^2)	C (N/m^2)	δ
700	1000	700	1400	17
A_d (N/m^2)	β	ϕ_o	ϕ	B (m)
39	35	30	30	0.0127
H (m)	R (m)	θ	α	v (m/s)
D+ 0.1	10000	0.001	89	0.0033

4.5. *Validating solutions with experimental data*

In the literature, various force models were compared with the experimental data to determine the accuracy of the cutting force at various cutting depths. These models were tested for different types of soil, blades and operating conditions in their respective studies. In King, Susante, and Gefreh (2011), many force models were compared on two types of soil and the same set of bulldozer and bulldozer blade. For validating the multi-objective formulation, NSGA-II is run for the given set of parameters for soil, blade, and bulldozer, which are given in Table 4. NSGA-II parameters are kept same. $F_{max}$is set as 0.05 kN and P_{dmin} is set as 0.02 m^3/s. It can be seen from Figure 7 that the obtained PO solutions are closer to the experimental cutting force of King et al. (2011). It concludes that the proposed multi-objective formulation can be used in practice for determining the optimal solution and condition for a bulldozer and its blade in soil cutting.

5. Conclusion

A multi-objective approach was adopted in this paper, and the soil cutting operation for bulldozer and its blade was formulated with three objectives and three problem-specific constraints. The proposed formulation targeted an economic and productive soil cutting operation. A hybrid multi-objective evolutionary algorithm was used in which the local searches were executed on few non-dominated solutions by using the $\varepsilon-$ constraint method. The obtained solutions were validated with the experimental data from the literature. The post-optimal analysis revealed that two variables showed commonality for generating the PO solutions. Other decision variables presented relationships for trade-off among the objectives. With these results, some guidelines were suggested for a practitioner that can be used for making decisions in practice. With many useful outcomes from this paper, a survey can be carried out for adapting the proposed formulation and the post-optimal analysis in practice in consultation with the practitioners.

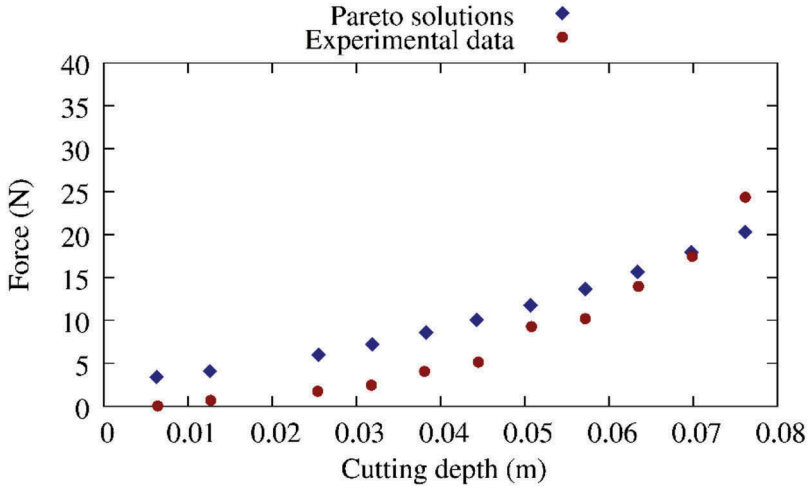

Figure 7. A close agreement between obtained PO solutions with the experimental data of King et al. (2011) is presented.

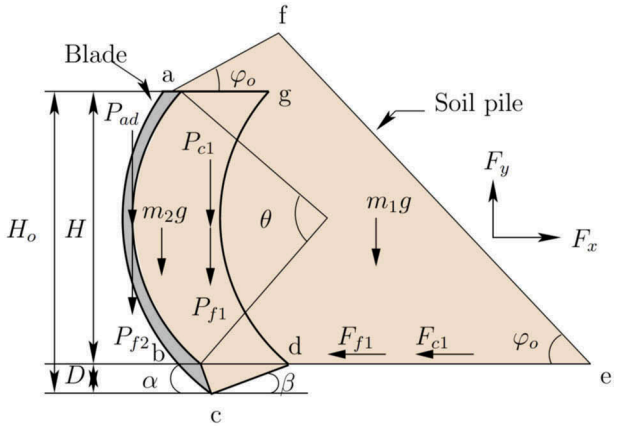

Figure 8. Forces acting on the blade (Sharma & Barakat, 2018).

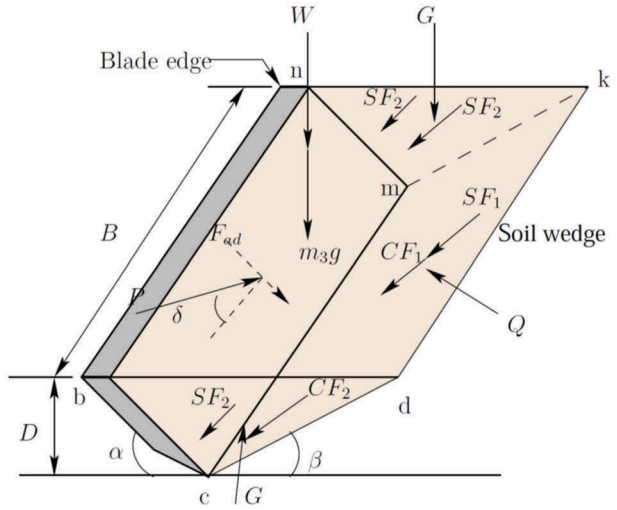

Figure 9. Forces acting on the soil wedge (Sharma & Barakat, 2018).

References

Abo-Elnor, M., Hamilton, R., & Boyle, J. T. (2004). Simulation of soil-blade interaction for sandy soil using advanced 3D finite element analysis. *Soil and Tillage Research*, *75*(1), 61–73.

Armin, A., Fotouhi, R., & Szyszkowski, W. (2014). On the FE modeling of soil-blade interaction in tillage operations. *Finite Elements in Analysis and Design*, *92*, 1–11.

Baishya, N. J., Sharma, D., & Dixit, U. S. (2014). Optimization of pressure vessel under thermo-elastic condition. *Journal of the Institution of Engineers (India): Series C*, *95*(4), 389–400.

Barakat, N., & Sharma, D. (2017a). Evolutionary bi-objective optimization of soil cutting by bull-dozer: A real-world application. *2017 International Conference on Advances in Mechanical, Industrial, Automation and Management Systems (AMIAMS)* (pp. 80–87). Allahabad. 2017. doi:10.1109/AMIAMS.2017.8069193

Barakat, N., & Sharma, D. (2017b). Modelling and bi-objective optimization of soil cutting and pushing process for bulldozer and its blade. *Journal of the Institution of Engineers (India): Series C*. doi:10.1007/s40032-017-0421-7

Barakat, N., & Sharma, D. (2017c). Towards optimal soil cutting process using a multi-objective genetic algorithm. *A National Conference on Sustainable Mechanical Engineering: Today and Beyond (SMETB 2017)* (pp. 1–11).

Bentaher, H., Ibrahmi, A., Hamza, E., Hbaieb, M., Kantchev, G., Maalej, A., & Arnold, W. (2013). Finite element simulation of moldboard-soil interaction. *Soil and Tillage Research*, *134*, 11–16.

Coello Coello, C. A., Lamont, G. B., & Veldhuizen, D. A. V. (2007). *Evolutionary algorithms for solving multi-objective problems*. New York, NY: Springer.

Deb, K. (2001). *Multi-objective optimization using evolutionary algorithms* (1st ed.). Chichester, UK: Wiley.

Deb, K., Miettinen, K., & Sharma, K. (2009). A hybrid integrated multi-objective optimization procedure for estimating nadir point. *The proceeding of Evolutionary Multi-Criterion Optimization (EMO)* (pp. 569–583), April 07-10, 2009. Nantes, France.

Deb, K., Pratap, A., Agarwal, S., & Meyarivan, T. (2002). A fast and elitist multi-objective genetic algorithm: NSGA-II. *IEEE Transactions on Evolutionary Computation*, *6*(2), 182–197.

Deb, K., & Srinivasan, A. (2006). Innovization: Innovating design principles through optimization. *Proceedings of the Genetic and Evolutionary Computation Conference (GECCO-2006)* (pp. 1629–1636). New York: The Association of Computing Machinery (ACM).

Hettiaratchi, D. R. P., & Reece, A. R. (1967). Symmetrical three-dimensional soil failure. *Journal of Terramechanics*, *4*(3), 45–67.

King, R. H., Susante, P. V., & Gefreh, M. A. (2011). Analytical models and laboratory measurements of the soil–blade interaction force to push a narrow tool through JSC-1A lunar simulant and Ottawa sand at different cutting depths. *Journal of Terramechanics*, *48*(1), 85–95.

Kumar, A., Sharma, D., & Deb, K. (2007). A hybrid multi-objective optimization procedure using PCX based NSGA-II and sequential quadratic programming. *The proceedings of IEEE Congress on Evolutionary Computation (CEC)* (pp. 3011–3018). September 25-28, 2007. Singapore.

McKyes, E. (1985). *Soil Cutting and Tillage*. New York: Elsevier.

Miettinen, K. (1998). *Nonlinear Multiobjective Optimization* (Vol. 12, 1 ed.).International Series in Operations Research & Management Science. New York, NY: Springer.

Qinsen, Y., & Shuren, S. (1994). A soil-tool interaction model for bulldozer blades. *Journal of Terramechanics*, *31*(2), 55–65.

Reece, A. R. (1964). The fundamental equation of earth-moving mechanics. *Proceedings of the Institution of Mechanical Engineers*, *179*, 16–22.

Sharma, D. (2010). On the flexible applied boundary and support conditions of compliant mechanisms using customized evolutionary algorithm. *Proceedings of Simulated Evolution and Learning - 8th International Conference, SEAL 2010* (pp. 105–114). Springer. doi:10.1007/978-3-642-17298-4_11

Sharma, D., & Barakat, N. (2018). Evolutionary Bi-Objective optimization for bulldozer and its blade in soil cutting. *Journal of the Institution of Engineers (India): Series C*. doi:10.1007/s40032-017-0437-z

Sharma, D., Kumar, A., Deb, K., & Sindhya, K. (2007). Hybridization of SBX based NSGA-II and sequential quadratic programming for solving multi-objective optimization problems. *The proceedings of IEEE Congress on Evolutionary Computation (CEC)* (pp. 3003–3010). September 25-28, 2007. Singapore.

Shmulevich, I., Asaf, Z., & Rubinstein, D. (2007). Interaction between soil and a wide cutting blade using the discrete element method. *Soil and Tillage Research*, *97*(1), 37–50.

Sindhya, K., Miettinen, K., & Deb, K. (2013). A hybrid framework for evolutionary multi-objective optimization. *IEEE Transaction on Evolutionary Computation*, *17*(4), 495–511.

Tsuji, T., Nakagawa, Y., Matsumoto, N., Kadono, Y., Takayama, T., & Tanaka, T. (2012). 3D-DEM simulation of cohesive soil-pushing behavior by bulldozer blade. *Journal of Terramechanics*, *49*(1), 37–47.

Appendix

Cutting Force Model

Qinsen and Shuren (1994) developed the analytical model wherein the cutting force is determined when the wide blade of the bulldozer becomes fully loaded with soil. Various forces considered in this model are shown in Figure 8 which are explained in the following paragraphs.

(1) The forces generated by the soil pile (*fgde*) moving on the ground

(a) Weight of the soil pile on the ground is given as,

$$m_1 g = \frac{1}{2}\gamma_o B\left(H + 2D\tan\varphi_o\right)^2 \cot\varphi_o. \tag{11}$$

where γ_o is the density of cut soil, and φ_o is the angle of accumulation of cut soil.

(b) Frictional force between the soil pile and the ground is given as,

$$F_{f1} = m_1 g \tan\varphi. \tag{12}$$

where φ is the angle of internal friction.

(c) Cohesion force between the soil pile and the ground is given as,

$$F_{c1} = C_O\, B\big(H + 2D\tan\varphi_o\big). \tag{13}$$

where C_O is the cohesion of cut soil.

(2) The forces generated by the cut soil (*abdgf*) sliding up between the blade and the soil pile (*fgde*)

(a) Frictional force between the cut soil and soil pile is given as,

$$P_{f1} = \big(F_{f1} + F_{C1}\big)\tan\varphi \tag{14}$$

(b) Cohesion force between the cut soil and soil pile is given as,

$$P_{c1} = C_O BR\theta \tag{15}$$

(c) Adhesion force between the cut soil and blade is given as,

$$P_{ad} = A_d BR\theta \tag{16}$$

where A_d is the adhesion factor of soil-metal.

(d) Frictional force between the cut soil and blade is given as,

$$P_{f2} = \big(F_{f1} + F_{C1}\big)\tan\delta \tag{17}$$

where δ is the angle of soil-metal friction.

(e) Weight of the cut soil sliding upon the surface of blade is given as,

$$m_2 g = 2\gamma_O BHD \tag{18}$$

Other forces that are acting on the soil wedge at the failure zone are shown in Figure 9. The following is the description of the forces.

(1) The forces generated on the sides of soil wedge

(a) Force acting normal to the faces (bcd) and (nmk) of the soil wedge is calculated as,

$$G = \frac{1}{6}\gamma D^3(1-\sin\varphi)(\cot\alpha+\cot\beta) \tag{19}$$

where γ is the density of uncut soil, $\alpha$is the angle of cutting blade, and β is the angle that the rupture makes with the horizontal

(b) Frictional force on the sides (bcd) and (nmk) of the soil wedge is calculated as,

$$SF_2 = G\ tan\ \varphi \tag{20}$$

where G is the force acting normal to the face (bcd) and (nmk) of soil wedge.

(c) Cohesion force on the sides (bcd) and (nmk)of the soil wedge is calculated as,

$$CF_2 = \frac{1}{2}CD^2(\cot\alpha+\cot\beta) \tag{21}$$

(2) Other forces on the soil wedge

(a) Weight of soil wedge (bcdnmk),

$$\mathrm{m_3 g} = \frac{1}{2}\gamma \mathrm{BD}^2(\cot\alpha+\cot\beta) \tag{22}$$

(b) Adhesion force between the soil and cutting edge of the blade is given as,

$$\mathrm{F_{ad}} = \frac{\mathrm{A_d}}{\sin\alpha}\mathrm{BD} \tag{23}$$

Thus, the force acting normal to the face (bdkn) of the soil wedge is calculated as,

$$\mathrm{W} = \mathrm{P_{f1}} + \mathrm{P_{f2}} + \mathrm{P_{ad}} + \mathrm{m_2 g} + \mathrm{m_3 g} \tag{24}$$

(3) Forces on the rupture plane (bdkn)

(a) Cohesion force on the rupture plane is calculated as,

$$CF_1 = \frac{C}{\sin\beta}\ BD \tag{25}$$

(b) Frictional force on the rupture plane is calculated as,

$$SF_1 = Q\tan\varphi \tag{26}$$

The force acting on the cutting edge of the blade is given as,

$$P_r = \frac{W\sin(\beta+\varphi) - F_{ad}\cos(\alpha+\beta+\varphi) + 2\,SF_2\cos(\varphi) + 2\,CF_2\cos(\varphi) + CF_1\cos(\varphi)}{\sin(\alpha+\beta+\varphi+\delta)} \tag{27}$$

The horizontal component of the resultant force acting on the blade is determined as,

$$\mathrm{F_x} = \mathrm{P_r}\sin(\alpha+\delta) + \mathrm{F_{f1}} + \mathrm{F_{c1}} \tag{28}$$

The vertical component of the resultant force acting on the blade is determined as,

$$\mathrm{F_y} = \mathrm{P_r}\cos(\alpha+\delta) - (\mathrm{P_{f2}} + \mathrm{P_{ad}}) \tag{29}$$

Therefore, the resultant cutting force on the blade is calculated as,

$$\mathrm{F} = \sqrt[2]{\mathrm{F_x^2} + \mathrm{F_y^2}} \tag{30}$$

which is used for determining the first objective function of power.